MAIGO2 Is Involved in Exit of Seed Storage Proteins from the Endoplasmic Reticulum in *Arabidopsis thaliana* [W][OA]

Lixin Li,[a] Tomoo Shimada,[a] Hideyuki Takahashi,[a] Haruko Ueda,[a] Yoichiro Fukao,[a,b] Maki Kondo,[c] Mikio Nishimura,[c] and Ikuko Hara-Nishimura[a,1]

[a] Graduate School of Science, Kyoto University, Sakyo-ku, Kyoto 606-8502, Japan
[b] Graduate School of Biological Sciences, Nara Institute of Science and Technology, Ikoma 630-0101, Japan
[c] Department of Cell Biology, National Institute for Basic Biology, Okazaki 444-8585, Japan

Seed storage proteins are synthesized on the endoplasmic reticulum (ER) as precursors and then transported to protein storage vacuoles, where they are processed into mature forms. Here, we isolated an *Arabidopsis thaliana* mutant, *maigo2* (*mag2*), that accumulated the precursors of two major storage proteins, 2S albumin and 12S globulin, in dry seeds. *mag2* seed cells contained many novel structures, with an electron-dense core that was composed of the precursor forms of 2S albumin. 12S globulins were segregated from 2S albumin and were localized in the matrix region of the structures together with the ER chaperones lumenal binding protein and protein disulfide isomerase, which were more abundant in *mag2* seeds. The *MAG2* gene was identified as At3g47700, and the MAG2 protein had a RINT-1/TIP20 domain in the C-terminal region. We found that some MAG2 molecules were peripherally associated with the ER membrane. MAG2 had an ability to bind to two ER-localized t-SNAREs (for target-soluble NSF [*N*-ethylmaleimide–sensitive fusion protein] attachment protein receptor; At Sec20 and At Ufe1). Our findings suggest that MAG2 functions in the transport of storage protein precursors between the ER and Golgi complex in plants.

INTRODUCTION

Higher plants accumulate large quantities of storage proteins, such as globulins and albumins, in the protein storage vacuoles (PSVs) of dry seeds as a nitrogen source for growth after germination. These storage proteins are actively synthesized on the rough endoplasmic reticulum (ER) as precursor forms and then are transported into PSVs during seed maturation. Multiple pathways are predicted for the transport of storage proteins (reviewed in Harasaki et al., 2005; Jolliffe et al., 2005; Vitale and Hinz, 2005). However, despite much effort, the molecular mechanism underlying the vacuolar targeting of storage proteins has not yet been revealed.

Previously, we found an ER-derived compartment that accumulates precursors of storage proteins to be transported to PSVs in maturing pumpkin (*Cucurbita maxima*) seeds (Hara-Nishimura et al., 1993a) and designated it a PAC (for precursor-accumulating) vesicle (Hara-Nishimura et al., 1998). The PAC vesicles with diameters of ∼300 nm are composed of the aggregates of storage protein precursors that are energetically synthesized on the ER of pumpkin (Hara-Nishimura et al., 1993a), castor bean (*Ricinus communis*) (Hara-Nishimura et al., 1998), soybean (*Gly-*
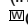
cine max) (Mori et al., 2004), and rice (*Oryza sativa*) (Takahashi et al., 2005). The PAC vesicles are involved in the efficient transport of the precursors of not only storage proteins but also a membrane protein (Mitsuhashi et al., 2001) into PSVs. PAC vesicles mediate an aggregation sorting of vacuolar proteins (reviewed in Hara-Nishimura et al., 2004).
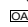
A proteomic analysis of the PAC vesicles isolated from maturing pumpkin seeds identified a type I integral membrane protein, PV72, on the PAC vesicle membrane (Shimada et al., 1997). An *Arabidopsis thaliana* mutant that lacks a PV72 homolog (At VSR1) partially missorts the storage proteins and secretes them out of the cells (Shimada et al., 2003a). Both PV72 and At VSR1 have an ability to bind to a vacuolar targeting signal of 2S albumin in a Ca-dependent manner (Shimada et al., 2002; Watanabe et al., 2002). These in vivo and in vitro analyses demonstrated that At VSR1/PV72 is a vacuolar sorting receptor (Shimada et al., 2003a; Hara-Nishimura et al., 2004; Watanabe et al., 2004).

It is unknown how the vacuolar sorting receptor functions in the intracellular transport of storage proteins. Most of the precursor molecules form an aggregate within the ER as described above. Some free molecules that are not incorporated into the aggregates should leave the ER for the Golgi complex, where they might be trapped by the vacuolar sorting receptor and recruited to the PAC vesicles (Hara-Nishimura et al., 2004). Selective uptake of the storage protein precursors into the PAC vesicles might occur in two ways: by aggregate sorting from the ER and by receptor-dependent sorting from the Golgi complex. The former sorting mechanism is advantageous to maturing seeds that actively synthesized a large quantity of storage proteins. The latter ensures proper delivery of the proteins by avoiding the missorting of the escaped molecules.

The PAC vesicle is unique to plants. However, the vacuolar targeting of storage proteins should involve vesicle transport, which is a basic process for protein delivery in yeast, mammals, and plants. Some mechanisms underlying vesicle transport are thought to be conserved in these organisms. The generation of transport vesicles requires cytosolic factors called coat proteins or coat-omers, which surround the resulting vesicles. The coat is removed immediately after the vesicles have formed to prepare the vesicles for fusing with their specific target membrane (Rothman and Orci, 1992). The initial contact between vesicles and target membranes is mediated by tethering factors (Barlowe, 1997; Cao et al., 1998). Then the vesicles proceed to the docking stage, which involves t-SNARE (for target-soluble NSF [N-ethylmaleimide–sensitive fusion protein] attachment protein receptor) proteins that interact in specific combinations to bring the vesicle and acceptor membranes into close proximity and promote their fusion.

To better understand the molecular mechanism underlying vacuolar targeting in plants, we screened for *Arabidopsis* mutants that abnormally accumulated the precursors of storage proteins and succeeded in isolating a mutant (designated *maigo2* [*mag2*]) that has a defect in the exit of storage proteins from the ER. The *MAG2* gene was identified and shown to encode a novel protein homologous with the mammalian RINT-1 and yeast Tip20p proteins. Our findings suggest that MAG2 is involved in the exit of storage protein precursors from the ER.

RESULTS

Arabidopsis mag2 Mutants Have a Defect in Vacuolar Targeting of Storage Proteins

To isolate *Arabidopsis* mutants that have a defect in the intra-cellular transport to the PSV, we screened the seeds of 28,000 T-DNA–tagged lines with antibodies that specifically react with the major storage proteins, 12S globulin and 2S albumin. Finally, we obtained eight mutant lines that abnormally accumulated precursors of these storage proteins and designated them *maigo* (*mag*) mutants (*maigo* means a stray child in Japanese). We focused on two of them that were found to be allelic by complementation test (data not shown). Figure 1A shows the immunoblot pattern of dry seeds from the two lines, *mag2-1* and *mag2-2*. Both mutant seeds accumulated the precursors of 12S globulin and 2S albumin, whereas wild-type (Columbia [Col-0]) seeds did not.

Figure 1B shows whole protein profiles of the mutant and wild-type seeds. The *mag2* seeds abnormally accumulated 54-, 51-, 49-, and 17-kD proteins in addition to the mature storage proteins. The N-terminal amino acid sequences of the 54- and 17-kD proteins were determined and found to correspond to the sequences immediately after the cotranslational cleavage sites of the signal peptides of the 12S globulin (12S1) and 2S albumin (2S3), respectively (Figure 1C). On the basis of the molecular masses, the 54- and 17-kD proteins were determined to be the proprotein precursors of 12S1 and 2S3, respectively. Similarly, the 51- and 49-kD proteins should be the proprotein precursors of other 12S globulin homologs because of their immunoreactivity with anti-12S globulin antibodies. These results indicated that the maturation of storage proteins was abolished in *mag2* mutants.

The abnormal accumulation of precursors of 12S globulin and 2S albumin in *mag2* mutants could be attributable to a defect in the gene for vacuolar processing enzyme (VPE), which converts proprotein precursors of storage proteins into the mature form (Hara-Nishimura et al., 1991, 1993b; Shimada et al., 2003b). However, this does not seem to be the case, because a *VPE*-defective mutant, *vpe*, significantly accumulated 15-kD precursor (pro2S3) and 16-kD precursor (pro2S4), whereas *mag2* mutants accumulated a 17-kD precursor (pro2S3). This finding
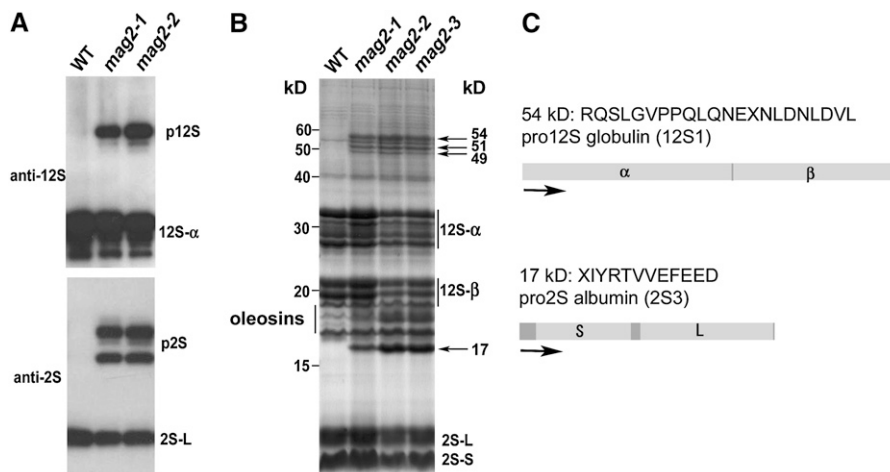

Figure 1. *mag2* Mutants Abnormally Accumulate the Precursors of Storage Proteins, 12S Globulins and 2S Albumins, in Seeds.

(A) Immunoblot of dry seeds of the wild type and *mag2* mutants with anti-12S globulin antibodies and anti-2S albumin antibodies. The *mag2* seeds accumulated large amounts of the precursors, pro12S globulin (p12S) and pro2S albumin (p2S), whereas wild-type seeds did not.
(B) Protein profiles of dry seeds (five grains) of the wild-type and *mag2* mutants. 12S-α and 12S-β, 12S globulin subunits; 2S-L and 2S-S, 2S albumin subunits.
(C) The N-terminal sequences of the 17- and 54-kD proteins that were accumulated in *mag2* mutants were determined. These sequences corresponded to the proprotein precursors of 12S globulin (12S1) and 2S albumin (2S3), respectively.

implies that *mag2* has a defect in vacuolar targeting of storage proteins rather than a defect in the *VPE* gene.

mag2 Seeds Develop a Large Number of Novel Structures with an Electron-Dense Core That Accumulates Storage Protein Precursors

Previously, we developed a method to see PSV morphology in dry seeds by detecting autofluorescence of PSVs with a laser-scanning confocal microscope (Shimada et al., 2003a). Using this method, we found that the sizes of the PSVs in *mag2* seeds were smaller than those in wild-type seeds (Figure 2A). The size reduction of PSVs might be caused by the abnormal targeting of storage proteins. *mag2* cells viewed with an electron microscope had smaller PSVs than did wild-type cells, resulting in a larger cytosolic space (Figure 2B). MAG2 might be responsible for the development of PSVs.

The most significant abnormality of *mag2* cells was a number of novel structures with a high electron-dense core inside, most of which were ~1 μm in diameter (Figure 2B). Interestingly, 2S albumin and 12S globulin were separately immunodetected in the structures of *mag2* seeds: 2S albumin was detected in the elec-tron-dense core, whereas 12S globulin was detected in the matrix region of the structures (Figure 2C). On the other hand, these two storage proteins were colocalized in PSVs of wild-type and *mag2* seeds (Figure 2C), suggesting that 2S albumin and 12S globulin are transported in an independent manner (see Discussion).

To determine the subcellular localization of the precursor proteins that were accumulated in the mutant seeds, we gener-ated specific antibodies against an N-terminal propeptide of 2S3, which is proteolytically removed by VPE (Shimada et al., 2003b). The antibodies (anti-2S3P) recognized the 2S albumin precur-sors but not the mature proteins (Figure 3A). Immunocytochem-istry with anti-2S3P antibodies clearly detected gold particles in the electron-dense core of the structures of *mag2-2* (Figures 3B and 3C). No gold particles were found in the matrix region or in PSVs of *mag2-2* (Figures 3B and 3C), indicating that the core of the *mag2* structures was composed of 2S albumin precursors.

mag2 Seeds Accumulate Higher Amounts of ER Chaperones in the Novel Structures

To identify the protein components that are abnormally accu-mulated in dry seeds of *mag2*, we performed two-dimensional
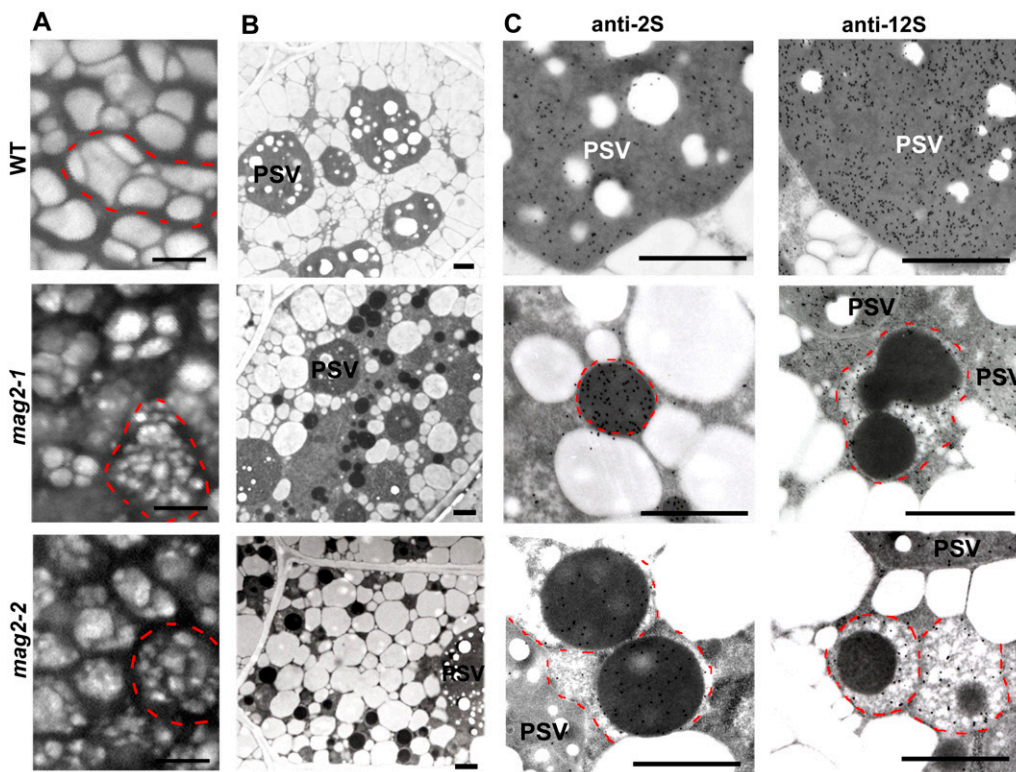

Figure 2. *mag2* Mutant Seeds Develop a Number of Novel Structures that Accumulate Storage Proteins.

(A) Autofluoresced PSVs in seeds of the wild type, *mag2-1*, and *mag2-2*. Each single cell is indicated by a dotted red line. *mag2* seeds have distorted cells and smaller PSVs than wild-type seeds.
(B) Electron micrographs of seed cells of the wild type, *mag2-1*, and *mag2-2*. Both *mag2-1* and *mag2-2* develop novel structures with an electron-dense core.
(C) Immunoelectron micrographs of wild-type, *mag2-1*, and *mag2-2* seeds with anti-2S and anti-12S antibodies. The novel structures in *mag2* mutants are surrounded by dotted red lines.
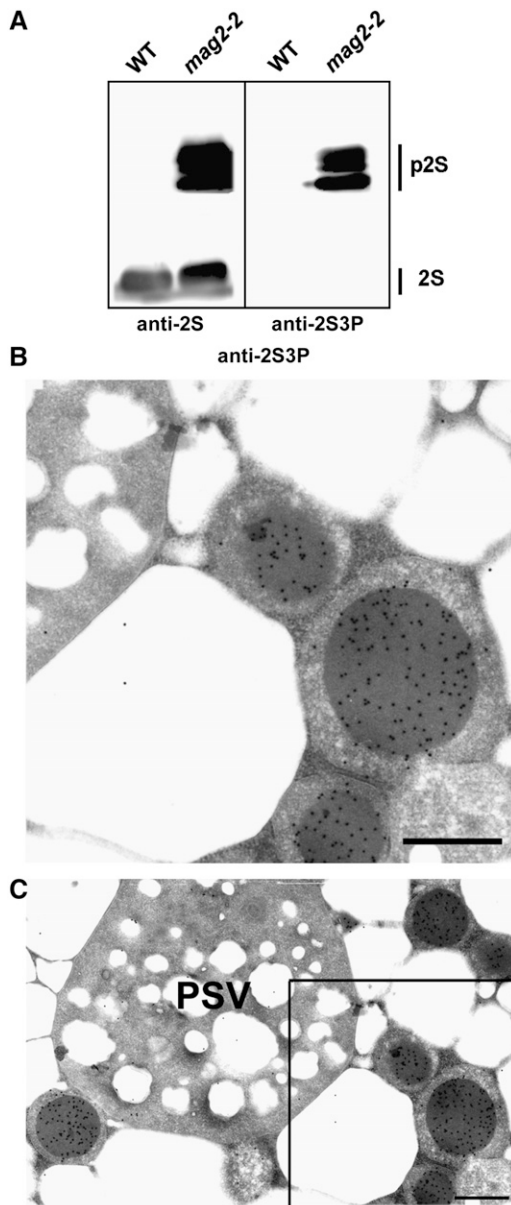Bars in **(A)** = 5 μm; bars in **(B)** and **(C)** = 1 μm.

A

Figure 3. Specific Localization of the 2S Albumin Precursors in the Electron-Dense Core of the Novel Structures in *mag2* Seeds.

(A) Immunoblot showing that anti-2S3P antibodies recognized 2S albumin precursors (p2S) but not the mature forms (2S). Dry seeds of wild-type and *mag2-2* plants were subjected to immunoblotting with anti-2S and anti-2S3P antibodies.

(B) and **(C)** Immunogold analysis of *mag2-2* seeds with anti-2S3P antibody, showing that 2S albumin precursors were localized in the electron-dense core of the structures but not in PSV. **(B)** shows a magnified image of the boxed area in **(C)**. Bars = 0.5 μm.

gel separation of proteins from wild-type and *mag2-1* seeds for a proteomic analysis. We examined 34 protein spots that exhibited visually different signal intensities on the gels after Coomassie blue staining (Figure 4). The proteins that were identified were categorized into six groups including storage proteins, ER-localized

molecular chaperones, and a late embryogenesis–abundant protein (Table 1). The late embryogenesis–abundant protein, which is thought to play a protective role in desiccation tolerance, was less abundant in *mag2* seeds.

Groups 1 and 2 consisted of the precursors of 12S globulins (12S1 to 12S4) and 2S albumins (2S1 to 2S4), respectively, that accumulated specifically in the *mag2-1* seeds. The precursors of 2S1, 2S2, and 2S4 were not detected on a one-dimensional gel because they were masked by bands of 18- to 19-kD oleosins (Figure 1). Oleosins could not be separated on a two-dimensional gel because of their hydophobicity. Group 3 included α-subunits of 12S globulins whose levels were reduced in *mag2-1*, in agreement with an immunoblot (Figure 1A). Group 4 included β-subunits of 12S globulins whose spot positions were more acidic in *mag2-1*. This observation suggests an abnormal processing of 12S globulins that is caused by missorting of processing enzymes in *mag2* seeds.

Group 5 included two ER-localized molecular chaperones, lumenal binding protein (BiP) of the Hsp70 family and protein disulfide isomerase (PDI), both of which were much more abundant in *mag2-1* seeds. The levels of BiP and PDI in *mag2* increased ∼16.6 and 6.2 times more than those of wild-type seeds, respectively. ER chaperones are known to increase when cells suffer from ER stress (Marocco et al., 1991; Martinez and Chrispeels, 2003; Kim et al., 2004; Kamauchi et al., 2005; Kirst et al., 2005). In *mag2*, there may be ER stress as a result of the abnormal accumulation of precursors of storage proteins (see Discussion).

In the wild type, the levels of BiP and ER-localized Hsp90 (referred to as GRP94 by Ishiguro et al., 2002) gradually increased during seed maturation and then decreased rapidly at the late stage, whereas in *mag2-1*, they did not decrease at the late stage, resulting in the accumulation of much higher amounts (Figure 5C). The level of PDI in the wild type also increased during seed maturation and then decreased slightly at the late stage, whereas in *mag2-1* it increased more rapidly and remained at a high level (Figure 5C).

In *mag2-3* seeds, BiP and PDI (Figure 5A) and 12S globulin (Figure 2C) were colocalized in the matrix region of the *mag2* structures, which suggests that the structures are derived from the ER. This was supported by the finding that some of them were surrounded by ribosomes (Figure 5B). Because ER chaperones have been shown to be constitutively transported to vacuoles to be degraded (Tamura et al., 2004), the relatively high levels of ER chaperones in *mag2* may arise because the chaperones cannot be transported to PSVs. If this is the case, MAG2 may function in the export step of storage protein precursors from the ER.

Identification of *MAG2*, a Gene That Encodes a Protein That Is Expressed Transiently at the Middle Stage of Seed Development

We found that *mag2-1* had a T-DNA at the 5′ untranslated region (12 bp upstream from the putative initiation codon) of At3g47700 and that *mag2-2* had a T-DNA in the intergenic region between At3g47730 and At3g47740 (Figure 6A). PCR-based analysis revealed a large deletion (at least ∼10 kb) from At3g47700 to At3g47730 in *mag2-2*. These results indicate that the *MAG2* gene is At3g47700, which consists of four exons and three introns.
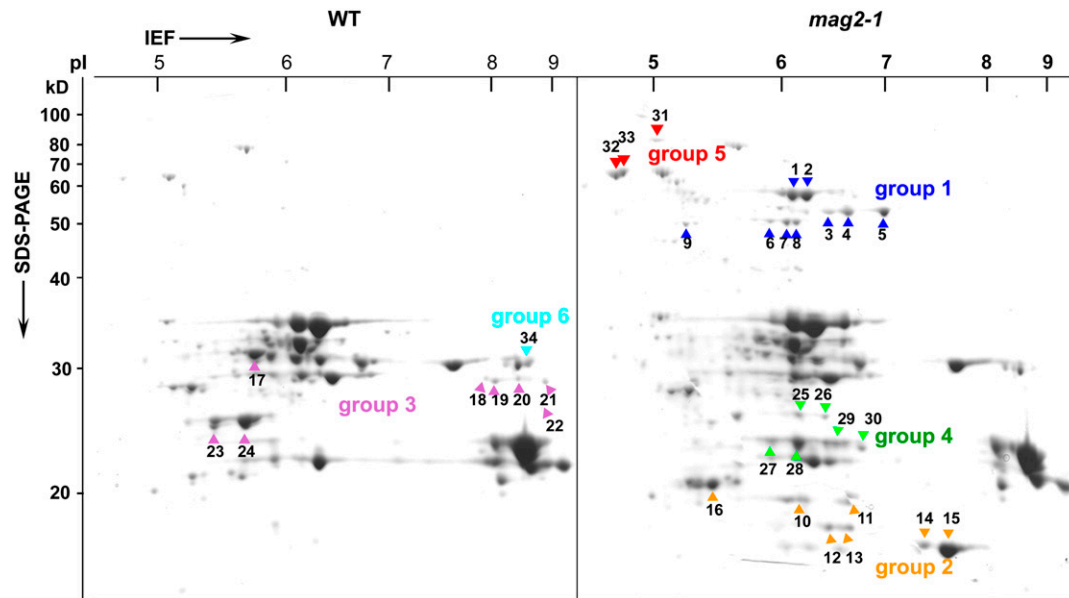
Figure 4. *mag2* Seeds Accumulate Not Only Storage Protein Precursors but Also Higher Amounts of ER Chaperones than Wild-Type Seeds.

Dry seeds of wild-type and *mag2-1* plants were subjected to two-dimensional electrophoresis followed by Coomassie blue staining. Differently accumulated proteins in these seeds were identified by matrix-assisted laser-desorption ionization time-of-flight mass spectrometry and separated into six groups (listed in Table 1). *mag2-1* seeds accumulated higher amounts of proteins of four groups (1, 2, 4, and 5) than wild-type seeds and accumulated lower amounts of proteins of two groups (3 and 6). Group 5 includes ER chaperones: BiP and PDI.

We also isolated a third allele, *mag2-3*, in which a T-DNA was inserted in the fourth exon of At3g47700 (Figure 6A). *mag2-3* exhibited almost the same phenotypes (Figures 1 and 5). In addition to the three T-DNA–tagged alleles, nine nucleotide-substituted alleles, *mag2-4* to *mag2-12*, were isolated from the *Arabidopsis* TILLING Project, as shown in Figure 6A. *mag2-4* and *mag2-8* had a stop codon in the middle region of the *MAG2* gene, and the others had substituted amino acids in MAG2. *mag2-4* to *mag2-9* accumulated precursors of 12S globulin and 2S albumin, as did *mag2-1*, *-2*, and *-3*, whereas *mag2-10* to *mag2-12* did not significantly accumulate the precursors, as summarized in Figure 6B. The immunoblot patterns are given in Supplemental Figure 1 online. This result indicates that Ser-265, Val-330, Leu-348, and Arg-437 are essential for the function of MAG2.

Figure 7 shows an immunoblot of maturing seeds using antibodies against the latter half of the MAG2 protein, 12S globulin, and 2S albumin. Both storage proteins started to be accumulated from full-sized-embryo stages. MAG2 increased earlier than the storage protein accumulation and then decreased. The developmental changes of MAG2 were parallel with those of BiP (Figure 5C), providing further evidence that MAG2 is involved in the traffic of storage proteins.

MAG2 Is Peripherally Associated with the ER Membrane Surface

An immunoblot detected MAG2 in two subcellular fractions, the P100 (microsomal proteins) fraction and the S100 (mixed cytosolic and vacuolar soluble proteins) fraction (Figure 8A), suggesting that a part of MAG2 localizes on membranes and another

part in cytosol. To determine whether MAG2 is localized on the ER membrane, the microsomal fraction was subjected to sucrose density gradient fractionation in the presence of $MgCl_2$ or EDTA. MAG2 showed a magnesium-dependent density shift on the gradients in parallel with the ER marker BiP (Figure 8B). This result indicates that a part of MAG2 was associated with the ER. To determine how MAG2 was associated on the membrane, we extracted MAG2 from the microsomes under various conditions. MAG2 was extracted from the microsomal fraction by high-salt (NaCl), alkaline (pH 11), or Triton X-100 buffer (Figure 8C). This profile was different from that of an integral membrane protein, VAM3 (Figure 8C) (Uemura et al., 2004). This finding is consistent with a hydropathy plot analysis predicting that MAG2 has no transmembrane domain (data not shown). These results indicate that MAG2 is a peripheral membrane protein of the ER.

MAG2 Interacts with At Sec20 and At Ufe1

MAG2 is composed of 795 amino acids and has a consensus RINT-1/TIP20 (TIP1) domain that is found in the region from Trp-299 to the C terminus (according to the National Center for Biotechnology Information [NCBI] Conserved Domain Database and the pfam database) (Figure 6A). The sequences of MAG2, RINT-1, and Tip20p are aligned in Supplemental Figure 2 online. The yeast protein Tip20p, formerly called Tip1p, is an ER peripheral protein associated with ER-localized t-SNAREs, Sec20p and Ufe1p (Sweet and Pelham, 1993; Lewis and Pelham, 1996). The mammalian RINT-1 was reported to function in membrane trafficking between the ER and the Golgi complex and to interact

Table 1. Identified Proteins That Are Differentially Accumulated between Wild-Type and *mag2* Seeds as Shown in Figure 4

Group	Spot No.	Identified Protein	Arabidopsis Genome Initiative Code	Peptide Mass Fingerprinting Hit Peptides (Mascot Score)	Tandem Mass Spectrometry Hit Peptides (Mascot Score)	Classification
	1	12S seed storage protein (12S1)	At4g28520	5 (243)	4 (207)	
	2	12S seed storage protein (12S1)	At4g28520	5 (433)	5 (397)	
	3	12S seed storage protein (12S4)	At5g44120	3 (120)	3 (98)	
	4	12S seed storage protein (12S4)	At5g44120	3 (151)	3 (115)	Pro12S globulin
1	5	12S seed storage protein (12S4)	At5g44120	3 (152)	3 (122)	
	6	12S seed storage protein (12S3)	At1g03880	4 (69)	2 (38)	
	7	12S seed storage protein (12S3)	At1g03880	4 (39)	0	
	8	12S seed storage protein (12S3)	At1g03880	5 (300)	4 (255)	
	9	12S seed storage protein (12S2)	At1g03880	3 (134)	3 (109)	
	10	2S seed storage protein (2S2)	At4g27150	2 (167)	2 (138)	
	11	2S seed storage protein (2S2)	At4g27150	3 (225)	2 (188)	
	12	2S seed storage protein (2S4)	At4g27170	4 (252)	4 (209)	Pro2S albumin
2	13	2S seed storage protein (2S4)	At4g27170	3 (161)	3 (124)	
	14	2S seed storage protein (2S3)	At4g27160	4 (376)	4 (319)	
	15	2S seed storage protein (2S3)	At4g27160	3 (232)	3 (226)	
	16	2S seed storage protein (2S1)	At4g27140	1 (111)	1 (92)	
	17	12S seed storage protein (12S4)	At5g44120	3 (260)	3 (228)	
	18	12S seed storage protein (12S4)	At5g44120	4 (218)	4 (174)	
	19	12S seed storage protein (12S3)	At1g03880	5 (228)	4 (189)	12S globulin α-subunit
	20	12S seed storage protein (12S4)	At5g44120	2 (148)	2 (127)	
3	21	12S seed storage protein (12S4)	At5g44120	3 (198)	3 (173)	
	22	12S seed storage protein (12S1)	At4g28520	4 (137)	4 (102)	
	23	12S seed storage protein (12S1)	At4g28520	2 (185)	2 (171)	
	24	12S seed storage protein (12S1)	At4g28520	4 (273)	4 (231)	
	25	12S seed storage protein (12S1)	At4g28520	2 (183)	2 (168)	
	26	12S seed storage protein (12S1)	At4g28520	2 (172)	2 (158)	12S globulin β-subunit
	27	12S seed storage protein (12S1)	At4g28520	2 (332)	2 (309)	
4	28	12S seed storage protein (12S1)	At4g28520	2 (344)	2 (317)	
	29	12S seed storage protein (12S1)	At4g28520	2 (320)	2 (297)	
	30	12S seed storage protein (12S1)	At4g28520	2 (79)	2 (51)	
	31	Lumenal binding protein2 (BiP2)	At5g42020	2 (56)	2 (34)	
5	32	Protein disulfide isomerase1 (PDI1)	At1g21750	3 (68)	3 (44)	Chaperon
	33	Protein disulfide isomerase2 (PDI2)	At1g77510	4 (72)	3 (43)	
6	34	Late embryogenesis–abundant protein2	At3g15670	2 (106)	2 (86)	LEA

with BNIP1 and ZW10, which are the orthologs of yeast Sec20p and Dsl1p, respectively (Hirose et al., 2004).

The *Arabidopsis* proteins At Sec20, At Ufe1, and At ZW10 were predicted to be orthologs of yeast Sec20p and Ufe1p (Sanderfoot et al., 2000) and mammalian ZW10 (NCBI database), respectively. Using a yeast two-hybrid assay, we found that MAG2 interacted with both At Sec20 and At Ufe1 and that At Sec20 interacted with At Ufe1 (Figure 9A). In contrast with these interactions, we could not detect any interaction of At ZW10 with MAG2, At Sec20, or At Ufe1 (Figure 9A). These results are summarized in Figure 9B. The overall results suggest that MAG2 functions in membrane trafficking between the ER and the Golgi complex.

DISCUSSION

Identification of a Novel *Arabidopsis* Mutant That Abnormally Accumulates Storage Protein Precursors in Dry Seeds

Three mutants of higher plants have been shown to be deficient in the intracellular transport of storage proteins: *Arabidopsis at-vsr1* (Shimada et al., 2003a), *Arabidopsis mag1* (Shimada et al., 2006), and rice *esp2* (Takemoto et al., 2002). They also accumulate a large amount of precursors of storage proteins in their seeds, as do *mag2* mutants. The *mag2* mutants, however, exhibit different characteristics from these three mutants.
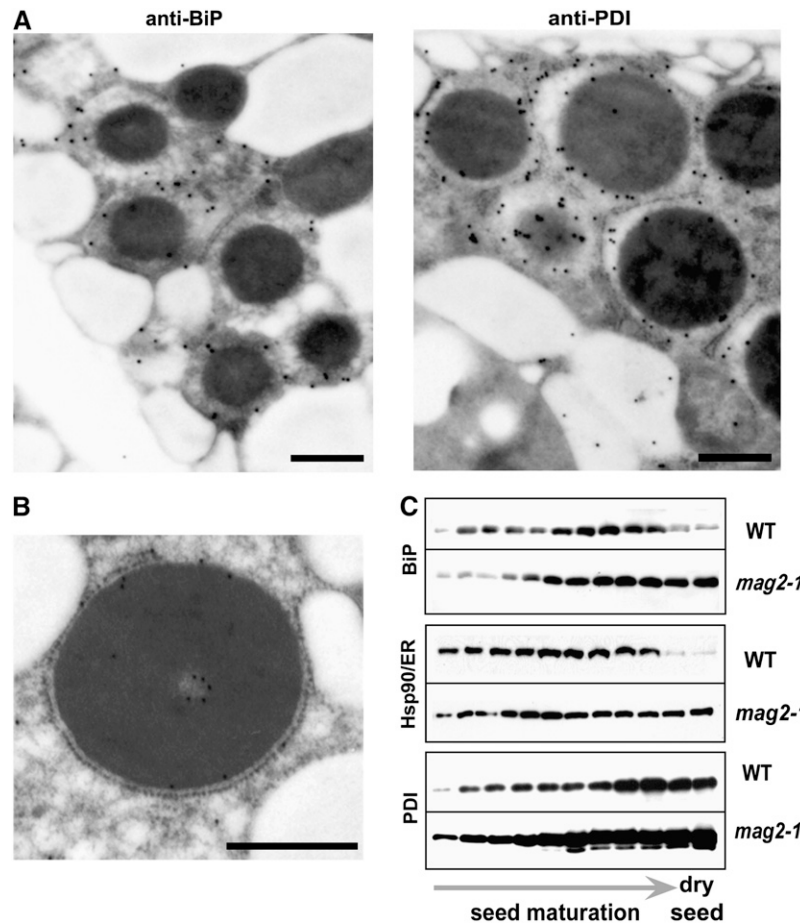
Figure 5. The Novel Structures of the *mag2* Mutant Accumulate ER Chaperones in the Matrix Region.

(A) Immunogold analysis of *mag2-3* seeds showing the localization of BiP and PDI in the matrix region of the novel structures. Bars = 0.5 μm.
(B) Immunoelectron micrograph of *mag2-2* seeds with anti-12S, showing the structure surrounded with ribosomes. Bar = 0.5 μm.
(C) Developmental changes in the levels of ER chaperones, including BiP, ER-localized Hsp90 (Hsp90/ER), and PDI, in maturing seeds of the wild type and *mag2-1*. Siliques at different developmental stages were alternately harvested starting from the top (just under the buds) of a wild-type plant.

First, cells of *mag2* do not secrete storage proteins, whereas cells of *Arabidopsis at-vsr1* (Shimada et al., 2003a) and *mag1* (Shimada et al., 2006) missort storage proteins by secreting them. At VSR1 is a member of the VSRs, which are unique to plants. Pumpkin VSR (PV72) and pea (*Pisum sativum*) VSR (BP-80) were found to directly bind to the vacuole-targeting signals of storage proteins (Kirsch et al., 1996; Shimada et al., 2002). We recently reported that MAG1 is At VPS29, a component of a retromer complex that is responsible for recycling At VSR1 from the prevacuolar compartment to the Golgi complex (Shimada et al., 2006). On the other hand, MAG2 might act between the ER and the Golgi complex, because (1) the *mag2* seeds contain a number of electron-dense structures that are derived from the ER (Figures 2, 3, and 5), (2) MAG2 interacts with ER-localized t-SNAREs (Figure 9), and (3) MAG2 is localized on the ER (Figure 8).

Second, rice *esp2* seeds develop irregularly shaped ER-derived compartments that contain the precursors of major storage proteins (glutelin and prolamin) (Takemoto et al., 2002). The ER-derived compartments are similar to the *mag2* structures in

that they are surrounded by ribosomes and have high electron density. However, the genes responsible for these mutations might be different from each other. Seeds of *esp2* had no detectable protein or mRNA of the ER-resident chaperone PDI, whereas *mag2* seeds accumulated much larger amounts of PDI than did wild-type seeds (Figures 4 and 5). *esp2* might develop ER-derived compartments composed of prolamin and proglutelin that are abnormally linked by disulfide bonds, because of the absence of PDI. *mag2* might develop the structures composed of the precursors, possibly because the precursors cannot leave the ER for the Golgi complex (see below). The abnormal accumulation of the precursors might cause ER stress, resulting in an increase of the levels of the molecular chaperones.

Another *mag2* structure–like compartment was reported in transgenic soybean seeds in which β-conglycinin expression was suppressed (Kinney et al., 2001). The compartment (designated an ER-derived protein body) is a pre-Golgi and nonvacuolar compartment and is composed of an electron-dense core of glycinin and its precursors.
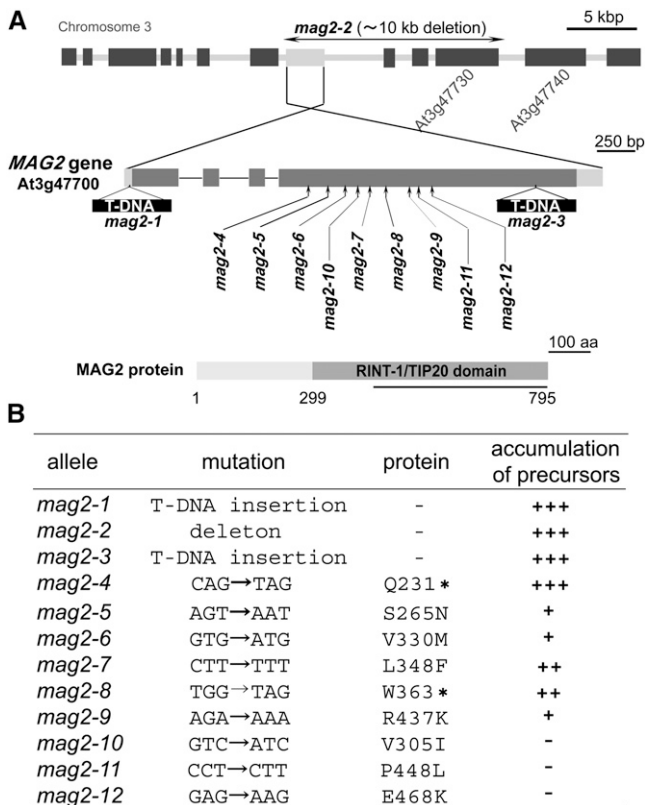
Figure 6. Identification of the *MAG2* Gene.

(A) The structure of the *MAG2* gene (At3g47700) and the mutation sites of *mag2* alleles. The *MAG2* gene consists of four exons (dark gray boxes) and three introns (solid lines). Two untranslated regions are indicated by light gray boxes. The T-DNA insertions in the *mag2-1* and *mag2-3* alleles and the large deletion in the *mag2-2* allele are shown. The MAG2 protein has a RINT-1/TIP20 domain in the C-terminal region. Anti-MAG2 antibodies were raised against the polypeptide corresponding to the latter half of the protein (solid line).

(B) Mutations and levels of storage protein precursors in *mag2* alleles. Asterisks indicate translation stops.

MAG2 Is Responsible for Protein Transport between the ER and the Golgi Complex

The *MAG2* gene was identified as At3g47700, whose protein product shares sequence similarity with Tip20p and RINT-1 (see Supplemental Figure 2 online). Mammalian RINT-1 is known as a G2/M checkpoint controlling factor (Xiao et al., 2001). RINT-1 is also reported to function in membrane trafficking from the ER to the Golgi complex in interphase cells (Hirose et al., 2004). Yeast Tip20p was reported to be involved in the retrograde transport from the Golgi complex to the ER. Cells of *tip20* mutants extensively accumulate ER membranes and vesicles as a result of inhibition of the retrograde transport (Sweet and Pelham, 1992). Inhibition of retrograde transport prevents the SNAREs and other factors that are necessary for anterograde transport from being retrieved to the ER, which in turn should inhibit anterograde transport.

Our finding that MAG2 interacts with At Sec20 and At Ufe1 (Figure 9) suggests that MAG2 functions as a complex with ER-localized SNAREs to facilitate the anterograde transport from the ER to the Golgi complex. Because the *mag2-4* and *mag2-8* mutants, each of which has a stop codon in the middle of the MAG2 gene, also accumulate storage protein precursors (Figure 6B; see Supplemental Figure 1 online), the RINT-1/TIP20 domain might be necessary for the formation of the functional complex of MAG2 and the SNAREs. However, MAG2 did not complement the temperature-sensitive phenotype of a *Saccharomyces cerevisiae* mutant lacking Tip20p (see Supplemental Figure 3 online), suggesting that it does not act as a functional homolog of yeast Tip20p. These results suggest that *mag2* has a defect in the anterograde transport of storage proteins from the ER to the Golgi complex. However, we cannot rule out the possibility that *mag2* has a defect in the retrograde transport from the Golgi complex to the ER for the reason mentioned above.

MAG2 is expressed in various organs in addition to maturing seeds (see Supplemental Figure 4 online). This fact implies that MAG2 is involved in the ER-to-Golgi transport of lytic vacuolar proteins in vegetative tissues. However, *mag2* mutants exhibit no abnormalities in seed germination or growth. *mag2* plants are morphologically indistinguishable from wild-type plants. In view of the importance of protein transport between the ER and the Golgi complex in various tissues, other factors may complement the lack of MAG2 in *mag2* mutants. The *Arabidopsis* genome database (NCBI, BLASTP2.2.12) shows that the At1g08400 protein has 33% identity and 52% similarity to MAG2. The At1g08400 protein (a MAG2 homolog) also contains the conserved RINT-1/TIP20 consensus domain, as does MAG2. This finding suggests that the MAG2 homolog has some complementary effects on the development of *mag2* plants.
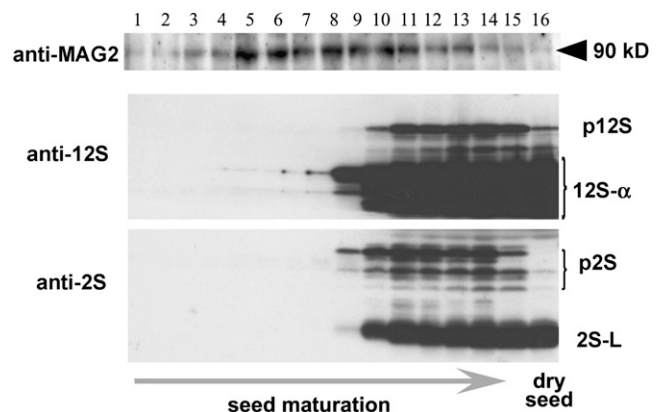

Figure 7. Developmental Changes in the Level of MAG2 during Seed Maturation.

Siliques at different developmental stages were alternately harvested starting from the top (just under the buds) of a wild-type plant. Maturing seeds from one silique were subjected to immunoblotting with anti-MAG2, anti-12S, and anti-2S antibodies. Storage proteins started to be accumulated from full-sized embryo stages. The MAG2 level increased earlier than the accumulation of storage proteins. p12S, pro12S globulin; p2S, pro2S albumin; 12S-α, 12S globulin α-subunit; 2S-L, 2S albumin large subunits.

On the other hand, although some storage proteins are accumulated as the precursor forms in the *mag2* structures, the other part of the storage proteins is normally transported and accumulated in PSVs. The MAG2 homolog could exhibit the complementary function in *mag2* seeds. Another possibility that cannot
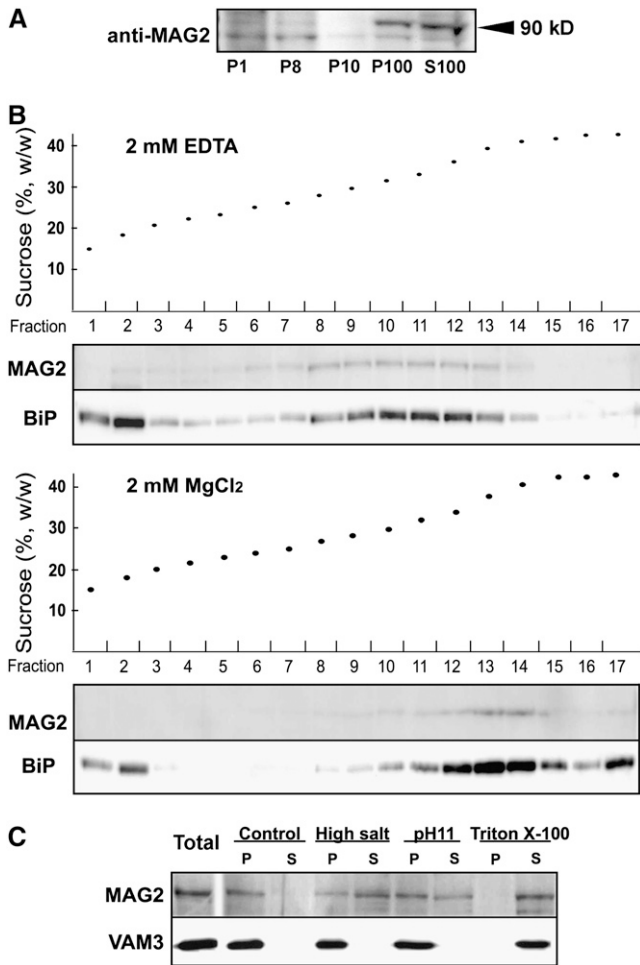

Figure 8. MAG2 Is Distributed on the ER Membrane and in the Cytosol.

(A) MGA2 is distributed on membrane and soluble fractions. Homogenate from a 10-d-old wild-type (Col-0) seedling was subjected to differential centrifugation to obtain the 1000*g* pellet (P1), the 8000*g* pellet (P8), the 10,000*g* pellet (P10), the 100,000*g* pellet (P100), and the 100,000 *g* supernatant (S100). Each fraction was subjected to immunoblotting with anti-MAG2 antibodies. MAG2 was distributed in P100 and S100 fractions.
(B) A part of MAG2 is localized on the ER. Microsomal fractions were prepared from 10-d-old wild-type (Col-0) seedlings in the presence of MgCl$_2$ or EDTA and subjected to sucrose density gradient (15 to 50%, w/v) centrifugation in the presence of MgCl$_2$ (bottom panel) or EDTA (top panel). Each fraction was subjected to immunoblot analysis with anti-MAG2 and anti-BiP antibodies.
(C) MAG2 is a peripheral membrane protein. Microsomal fractions from 11-d-old wild-type (Col-0) seedlings were resuspended in control buffer, high-salt buffer, alkaline (pH 11) buffer, and 1% Triton X-100 buffer. Suspensions were ultracentrifuged to obtain supernatant (S) and pellet (P) fractions. Each fraction was subjected to immunoblot analysis with anti-MAG2 and anti-VAM3 antibodies.
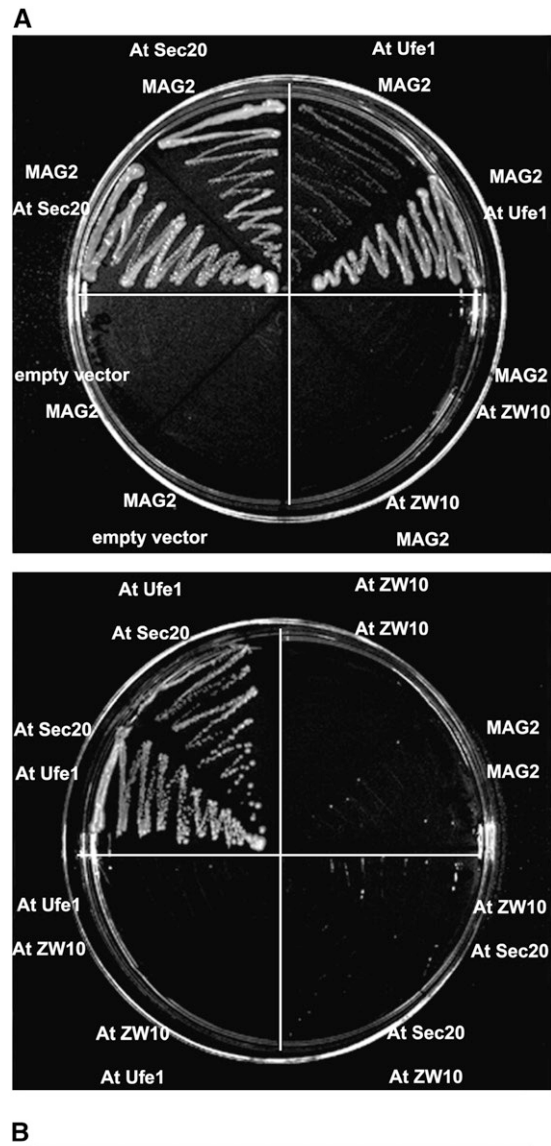

Figure 9. Interactions among MAG2, At Sec20, and At Ufe1.

(A) Yeast strain AH109 was transformed with the paired constructs for a fusion protein with the GAL4 activation domain (top panel) and a fusion protein with the GAL4 DNA binding domain (bottom panel). Transformants were streaked onto SD/−Leu/−Trp/−His/−Ade plates.
(B) Summary of the yeast two-hybrid analysis in **(A)**. AD, activation domain; BD, DNA binding domain; n.d., not determined.

BD \ AD	MAG2	At Sec20	At Ufe1	At ZW10
MAG2	-	++	+	-
At Sec20	++	n.d.	++	-
At Ufe1	++	++	n.d.	-
At ZW10	-	-	-	-

be excluded is that *Arabidopsis* has a MAG2-independent transport pathway for storage proteins.

We isolated two T-DNA–tagged lines that had a defect in the *MAG2* homolog gene. However, these T-DNA–tagged lines exhibited no phenotype and accumulated no precursors of storage proteins in the seeds (data not shown). It is possible that MAG2 is responsible for the complementary function of these mutants.

Vacuolar Targeting of Storage Proteins

The segregation of 2S albumin and 12S globulin within the *mag2* structures (Figure 2C) suggests that these proteins are delivered in an independent manner. The localization of 2S albumin precursor in the electron-dense core of the structures indicates that the 2S albumin precursors form aggregates more easily than the 12S globulin precursors. The formation of the aggregates might be facilitated by the increased levels of the storage proteins in the ER lumen of *mag2*, because of the inhibition of the transport between the ER and the Golgi complex.

The formation of the *mag2* structures resembles that of PAC vesicles in pumpkin maturing seeds in that both bodies are formed from aggregates of precursor proteins within the ER lumen. PAC vesicles may be responsible for the sorting of proteins to PSVs in the following manner: storage protein aggregates that form within the ER develop into the PAC vesicles and are directly incorporated into PSVs. In the *mag2* mutant, blocking the transport between the ER and the Golgi complex led to the aggregation of 2S albumin precursors and favored the formation of the *mag2* structures. However, unlike PAC vesicles in pumpkin, the *mag2* structures did not reach the PSVs in the *mag2* mutant. Thus, it is possible that MAG2 is involved in the budding of aggregates from the ER. Another possibility is that MAG2 is involved in the exit of the free molecules from the ER to the Golgi complex or in the retrograde transport from the Golgi complex to the ER. Further analysis is necessary to clarify whether a Golgi-independent aggregation-sorting pathway acts in maturing *Arabidopsis* seeds.

METHODS

Plant Materials

Arabidopsis thaliana ecotype Col-0 and Col *er*-105 were used as wild-type plants. T-DNA–tagged lines (*mag2-1* to *mag2-3*) were derived from Col-0, and nucleotide-substituted lines (*mag2-4* to *mag2-12*) were derived from Col *er*-105. *Arabidopsis* seeds were surface-sterilized and then sown on soil or onto 0.5% Gellan Gum (Wako) with Murashige and Skoog medium (Wako) and 1% (w/v) sucrose. Plants were grown at 22°C under continuous light.

We isolated two mutants (*mag2-1* and *mag2-2*) from *Arabidopsis* T-DNA–tagged lines. We obtained *mag2-3* (391C01) from a GABI-kat T-DNA–tagged population and *mag2-4* to *mag2-12* (stock numbers CS87076, CS94046, CS86176, CS85448, CS88591, CS86430, CS93495, CS93952, and CS92590) from the *Arabidopsis* TILLING project (http://tilling.fhcrc.org).

We obtained two T-DNA–tagged lines deficient in the MAG2 homolog (At1g08400): one is 288E12 from the GABI-kat T-DNA–tagged population, and the other is CS849783 from the *Arabidopsis* Knockout Facility at the University of Wisconsin-Madison.

Antibodies

To prepare antibodies against *Arabidopsis* 2S precursors (anti-2S3P) that do not recognize the mature form of 2S albumin, we chemically synthesized a peptide (SIYRTVVEFEEDDASNC) with a peptide synthesizer (model 431 A; Applied Biosystems). The peptide sequence was composed of the N-terminal propeptide of an *Arabidopsis* 2S albumin (2S3) and a Cys residue that was used as a linker for conjugation of the peptide to BSA with 3-maleimidobenzoic acid *N*-hydroxysuccinimide ester (Sigma-Aldrich). The peptide–BSA conjugates were injected into a rabbit to generate antibodies as described previously (Matsushima et al., 2003). The antibodies were purified before being used. Serum was injected onto an *N*-hydroxysuccinimide column (HiTrap NHS-activated HP; Amersham Biosciences) that had been conjugated with crude extract from Col-0 seeds, and the flow-through was collected to use for further analysis.

MAG2 cDNA was donated from the Riken BioResource Center (BRC) (Seki et al., 1998, 2002). For the preparation of anti-MAG2 antibodies, a DNA fragment corresponding to the MAG2 C-terminal half region from Leu-401 to the C terminus was inserted into pET32a vector (Novagen). Recombinant protein that was composed of the C-terminal half of MAG2, the His tag, and thioredoxin was expressed in *Escherichia coli* BL-21 (DE3) cells and purified with a HiTrap chelating column. We generated specific antibodies against MAG2 as described previously (Tamura et al., 2004). Because the antibodies cross-reacted nonspecifically with several bands on the immunoblot of total extract from *Arabidopsis* plants, we identified an ~90-kD single band on the blot of wild-type seeds but not of *mag2* seeds (data not shown).

We also used antibodies against either 12S globulin or 2S albumin that had been prepared (Shimada et al., 2003b), anti-BiP (aC-19; Santa Cruz Biotechnology), anti-PDI (Stressgen), and antibody against ER-localized Hsp90 that was donated by S. Ishiguro of Nagoya University.

Immunoblotting

SDS-PAGE and immunoblot analysis were performed as described previously (Shimada et al., 2003a). Dilutions of antibodies were as follows: anti-MAG2 (1:1000), anti-12S (1:20,000), anti-2S (1:10,000), anti-2S3P (1:5000), anti-BiP (1:1000), anti-PDI (1:10,000), antibody against ER-localized Hsp90 (1:1000), anti-VAM3 (1:5000) (Sato et al., 1997), and horseradish peroxidase–conjugated goat antibodies against rabbit IgG (1:5000; Pierce). Immunoreactive signals were detected with an enhanced chemiluminescence detection system (Amersham Biosciences).

Microscopic Analysis

Laser-scanning confocal microscopic analysis and immunoelectron microscopy with dry seeds were performed as described previously (Shimada et al., 2003a). Samples were treated with antibodies against 12S (dilution, 1:50), 2S (1:50), 2S3P (1:1000), BiP (1:1000), and PDI (1:200). Sections were examined with a transmission electron microscope (1200EX; JEOL) at 80 kV. We examined the seeds of all three alleles (*mag2-1*, *mag2-2*, and *mag2-3*) by electron microscopy and immunoelectron microscopy and found that they exhibited the same ultrastructure phenotypes.

Two-Dimensional Electrophoresis

Dry seeds (40 mg) from wild-type (Col-0) and *mag2-1* plants were ground in 2 mL of acetone. The supernatant was incubated at −20°C overnight and then centrifuged at 15,000 rpm and 4°C for 15 min. The pellet was suspended in 200 μL of reswelling buffer as described by Matsushima et al. (2004). After centrifugation at 15,000 rpm and 4°C for 15 min, the supernatant was subjected to two-dimensional electrophoresis as described previously (Matsushima et al., 2004). The levels of BiP and PDI were estimated by image analysis with Multi Gauge software (version 3.0; Fujifilm).

Mass Spectrometry

The two-dimensional gels were treated with Coomassie Brilliant Blue R 250, and protein spots that exhibited different accumulation between wild-type and *mag2-1* seeds were excised. Each spot was washed twice with 100 μL of 0.05 M NH_4HCO_3 in 50% (v/v) methanol for 20 min and then with 100 μL of 75% (v/v) acetonitrile for 20 min. Gel pieces were dried in an evaporator. Then, samples were digested with 0.2 μg of trypsin (Promega) in 20 μL of 0.02 M NH_4HCO_3 for 12 h at 37°C. The trypsin peptides were extracted from gel pieces with 20 μL of 5% (v/v) trifluoroacetic acid and twice by 50% (v/v) acetonitrile. The resulting solution that contained extracted peptides was dried with an evaporator. The dried sample was reconstituted by adding 3 μL of 0.1% trifluoroacetic acid and 50% (v/v) acetonitrile and gently pipetting up and down to dissolve the extracted peptides. The peptides were purified and concentrated with reverse-phase medium (C18 Zip-Tips; Millipore). The peptides and 150 ng of α-cyano-4-hydroxy-cinnamic acid (Bruker Daltonics) were mixed and subjected to peptide mass fingerprinting analysis by matrix-assisted laser-desorption ionization time-of-flight mass spectrometry (REFLEX III; Bruker Daltonics). Proteins were identified as the highest ranking result by a search of the NCBI database using Mascot (http://www. matrixscience.com/cgi/search). The search parameters allowed for carbamidomethylation of Cys, one miscleavage of trypsin, and 100 ppm mass accuracy.

Subcellular Fractionation

The fractionation was performed essentially as described previously (Tamura et al., 2005). Ten-day-old seedlings of wild-type plants (Col-0; 2.6 g fresh weight) were chopped with a razor blade in a Petri dish on ice in 1.1 mL of buffer A (50 mM HEPES-KOH, pH 7.5, 5 mM EDTA, 0.4 M sucrose, and protease inhibitor cocktail [Roche]). The homogenate was filtered through Cell Strainer (70 μm) by centrifugation at 500 rpm. An aliquot of the filtrate was used as a total fraction. One milliliter of the filtrate was centrifuged at 1000*g* and 4°C for 20 min. The pellet P1 was suspended in 1 mL of buffer A, and the supernatant was centrifuged at 8000*g* and 4°C for 20 min. The pellet P8 was suspended in 1 mL of buffer A, and the supernatant was centrifuged at 10,000*g* and 4°C for 20 min. The pellet P10 was suspended in 1 mL of buffer A, and the supernatant was ultracentrifuged at 100,000*g* and 4°C for 1 h. The pellet P100 was suspended in 1 mL of buffer A, and the volume of the supernatant (S100) fraction was measured. Each of total fractions, P1, P8, P10, P100, and S100, was subjected to immunoblot analysis with anti-MAG2 antibodies.

For suborganellar fractionation, the microsomal fractions were prepared from 10-d-old seedlings of wild-type plants (Col-0; 0.5 g fresh weight) in 2 mL of 2 mM $MgCl_2$ or 2 mM EDTA in buffer B (50 mM HEPES-KOH, pH 7.5, 1 mM EGTA, 0.4 M sucrose, and protease inhibitor cocktail [Roche]) after sequential centrifugations at 3000*g* for 20 min, 10,000*g* for 20 min, and 100,000*g* for 1 h. The microsomal fractions were resuspended in 0.5 mL of buffer B in the presence of 2 mM $MgCl_2$ or 2 mM EDTA and layered directly on top of a 16-mL linear sucrose density gradient (15 to 50%, w/v). Centrifugation was performed in an SW28.1 rotor (Beckman) at 25,000 rpm for 13 h at 4°C, and 1-mL fractions were collected with a piston gradient fractionator (TOWA LABO). Each fraction was concentrated with acetone and subjected an immunoblotting.

To perform suborganellar fractionation, each microsomal fraction that was prepared from 11-d-old seedlings of wild-type plants (0.09 g fresh weight) was resuspended in 600 μL of each solution of buffer A, high-salt buffer (1 M NaCl in buffer A), alkaline buffer (0.1 M Na_2CO_3, pH 11, in buffer A), and Triton X-100 buffer (1% [v/v] Triton X-100 in buffer A). After incubation for 20 min, these suspensions were ultracentrifuged at 100,000*g* for 1 h at 4°C to obtain supernatant and pellet fractions. Each fraction was subjected to immunoblotting.

Identification of the *MAG2* Gene

The *MAG2* gene was identified with genomic DNA from *mag2-1* leaves by thermal asymmetric interlaced PCR as described previously (Liu et al., 1995). Primers specific to the T-DNA border, pBI-TR-1 (5′-CGTCAGTG-GAGCATTTTTGACAAG-3′) and pBI-TR-2 (5′-TTTGCTAGCTGATAGT-GACCTTAG-3′), were used for the first and second amplifications, respectively. A degenerated primer, TAIL-1 (5′-[ATGC]GTCGA[GC][AT]-GA[ATGC]A[AT]GAA-3′), was also used. For DNA sequence of the resulting PCR products, pBI-TR-3 (5′-AAACTCCAGAAACCCGCGGCTGAG-3′) was used.

Yeast Two-Hybrid Assay

At *ZW10* cDNA was donated by the Riken BioResource Center (Seki et al., 1998, 2002). *GFP-SYP81* was donated by M.H. Sato (Kyoto Prefectural University). At *Ufe1/SYP81* was amplified using *GFP-SYP81* as a template. At *Sec20* cDNA was cloned from mRNAs of flower buds of *Arabidopsis*. A yeast two-hybrid assay was performed using the MATCH-MAKER kit (BD Biosciences). The cDNAs of *MAG2* and At *ZW10* were amplified and fused in-frame downstream of the GAL4 activation domain in the pGADT7 vector or downstream of the GAL4 DNA binding domain in the pGBKT7 vector. The DNA fragment for a cytosolic domain of At Sec20 or At Ufe1 was introduced into pGADT7 and pGBKT7 vectors. We introduced the paired constructs shown in Figure 9 into strain AH109 of *Saccharomyces cerevisiae* and selected on SD/−Leu/−Trp (Synthetic Defined plate deficient for both Leu and Trp) plates. The interactions were examined on SD/−Leu/−Trp/−His/−Ade plates.

Complementation Test of MAG2

cDNA of *MAG2* was inserted into pYES vector and introduced into *tip20-5* yeast cells, which were donated by M.J. Lewis of the Medical Research Council Laboratory of Molecular Biology. Transformed yeasts were selected on SD/−Uracil plates and then streaked onto YPDA plates for subsequent growth at 24 or 37°C. *TIP20* (PTM1), donated by M.J. Lewis, was used as a positive control.

Accession Numbers

GenBank/EMBL accession numbers and Arabidopsis Genome Initiative locus identifiers for the genes mentioned in this article are as follows: *MAG2*, At3g47700.1; At *Sec20*, At3g24315.1; At *Ufe1*, At1g51740.1; At *ZW10*, At2g32900; RINT-1, XM_778896; *TIP20*, gi 473556.

Supplemental Data

The following materials are available in the online version of this article.

Supplemental Figure 1. Accumulation Levels of the Precursors of Storage Proteins in Seeds of *mag2* Alleles Isolated by the TILLING Project.

Supplemental Figure 2. Alignment of Amino Acid Sequences of MAG2 (gi 4741187), Tip20p (gi 464886; *Saccharomyces cerevisiae*), and RINT-1 (gi 11967435; *Homo sapiens*).

Supplemental Figure 3. Complementation Test of the Yeast *tip20-5* Mutant with MAG2.

Supplemental Figure 4. Tissue-Specific Expression of the *MAG2* Gene.

ACKNOWLEDGMENTS

REFERENCES

Barlowe, C. (1997). Coupled ER to Golgi transport reconstituted with purified cytosolic proteins. J. Cell Biol. **139,** 1097–1108.

Cao, X., Ballew, N., and Barlowe, C. (1998). Initial docking of ER-derived vesicles requires Uso1p and Ypt1p but is independent of SNARE. proteins. EMBO J. **17,** 2156–2165.

Hara-Nishimura, I., Inoue, K., and Nishimura, M. (1991). A unique vacuolar processing enzyme responsible for conversion of several proprotein precursors into the mature forms. FEBS Lett. **294,** 89–93.

Hara-Nishimura, I., Matsushima, R., Shimada, T., and Nishimura, M. (2004). Diversity and functions of ER-derived compartments in plants: Are these compartments specific to plant cells? Plant Physiol. **136,** 3435–3439.

Hara-Nishimura, I., Shimada, T., Hatano, K., Takeuchi, Y., and Nishimura, M. (1998). Transport of storage proteins to protein-storage vacuoles is mediated by large precursor-accumulating vesicles. Plant Cell **10,** 825–836.

Hara-Nishimura, I., Takeuchi, Y., Inoue, K., and Nishimura, M. (1993a). Vesicle transport and processing of the precursor to 2S albumin in pumpkin. Plant J. **4,** 793–800.

Hara-Nishimura, I., Takeuchi, Y., and Nishimura, M. (1993b). Molecular characterization of a vacuolar processing enzyme related to a putative cysteine proteinase of *Schistosoma mansoni.* Plant Cell **5,** 1651–1659.

Harasaki, K., Lubben, N.B., Harbour, M., Taylor, M.J., and Robinson, M.S. (2005). Sorting of major cargo glycoproteins into clathrin-coated vesicles. Traffic **6,** 1014–1026.

Hirose, H., Arasaki, K., Dohmae, N., Takio, K., Hatsuzawa, K., Nagahama, M., Tani, K., Yamamoto, A., Tohyama, M., and Tagaya, M. (2004). Implication of ZW10 in membrane trafficking between the endoplasmic reticulum and Golgi. EMBO J. **23,** 1267–1278.

Ishiguro, S., Watanabe, Y., Ito, N., Nonaka, H., Takeda, N., Sakai, T., Kanaya, H., and Okada, K. (2002). SHEPHERD is the Arabidopsis GRP94 responsible for the formation of functional CLAVATA proteins. EMBO J. **21,** 898–908.

Jolliffe, N.A., Craddock, C.P., and Frigerio, L. (2005). Pathways for protein transport to seed storage vacuoles. Biochem. Soc. Trans. **33,** 1016–1018.

Kamauchi, S., Nakatani, H., Nakano, C., and Urade, R. (2005). Gene expression in response to endoplasmic reticulum stress in *Arabidopsis thaliana.* FEBS J. **272,** 3461–3476.

Kim, C.S., Hunter, B.G., Kraft, J., Boston, R.S., Yans, S., Jung, R., and Larkins, B.A. (2004). A defective signal peptide in a 19-kD alpha-zein protein causes the unfolded protein response and an opaque endosperm phenotype in the maize De*-B30 mutant. Plant Physiol. **134,** 380–387.

Kinney, A.J., Jung, R., and Herman, E.M. (2001). Cosuppression of the α subunits of β-conglycinin in transgenic soybean seeds induces the

formation of endoplasmic reticulum-derived protein bodies. Plant Cell **13,** 1165–1178.

Kirsch, T., Saalbach, G., Raikhel, N.V., and Beevers, L. (1996). Interaction of a potential vacuolar targeting receptor with amino- and carboxyl-terminal targeting determinants. Plant Physiol. **111,** 469–474.

Kirst, M.E., Meyer, D.J., Gibbon, B.C., Jung, R., and Boston, R.S. (2005). Identification and characterization of endoplasmic reticulum-associated degradation proteins differentially affected by endoplasmic reticulum stress. Plant Physiol. **138,** 218–231.

Lewis, M.J., and Pelham, H.R. (1996). SNARE-mediated retrograde traffic from the Golgi complex to the endoplasmic reticulum. Cell **85,** 205–215.

Liu, Y.G., Mitsukawa, N., Oosumi, T., and Whittier, R.F. (1995). Efficient isolation and mapping of *Arabidopsis thaliana* T-DNA insert junctions by thermal asymmetric interlaced PCR. Plant J. **8,** 457–463.

Marocco, A., Santucci, A., Cerioli, S., Motto, M., Di Fonzo, N., Thompson, R., and Salamini, F. (1991). Three high-lysine mutations control the level of ATP-binding HSP70-like proteins in the maize endosperm. Plant Cell **3,** 507–515.

Martinez, I.M., and Chrispeels, M.J. (2003). Genomic analysis of the unfolded protein response in Arabidopsis shows its connection to important cellular processes. Plant Cell **15,** 561–576.

Matsushima, R., Fukao, Y., Nishimura, M., and Hara-Nishimura, I. (2004). NAI1 gene encodes a basic-helix-loop-helix-type putative transcription factor that regulates the formation of an endoplasmic reticulum-derived structure, the ER body. Plant Cell **16,** 1536–1549.

Matsushima, R., Kondo, M., Nishimura, M., and Hara-Nishimura, I. (2003). A novel ER-derived compartment, the ER body, selectively accumulates a β-glucosidase with an ER-retention signal in Arabidopsis. Plant J. **33,** 493–502.

Mitsuhashi, N., Hayashi, Y., Koumoto, Y., Shimada, T., Fukasawa-Akada, T., Nishimura, M., and Hara-Nishimura, I. (2001). A novel membrane protein that is transported to protein-storage vacuoles via precursor-accumulating vesicles. Plant Cell **13,** 2361–2372.

Mori, T., Maruyama, N., Nishizawa, K., Higasa, T., Yagasaki, K., Ishimoto, M., and Utsumi, S. (2004). The composition of newly synthesized proteins in the endoplasmic reticulum determines the transport pathways of soybean seed storage proteins. Plant J. **40,** 238–249.

Rothman, J.E., and Orci, L. (1992). Molecular dissection of the secretory pathway. Nature **355,** 409–415.

Sanderfoot, A.A., Assaad, F.F., and Raikhel, N.V. (2000). The Arabidopsis genome. An abundance of soluble N-ethylmaleimide-sensitive factor adaptor protein receptors. Plant Physiol. **124,** 1558–1569.

Sato, M.H., Nakamura, N., Ohsumi, Y., Kouchi, H., Kondo, M., Hara-Nishimura, I., Nishimura, M., and Wada, Y. (1997). The AtVAM3 encodes a syntaxin-related molecule implicated in the vacuolar assembly in *Arabidopsis thaliana.* J. Biol. Chem. **272,** 24530–24535.

Seki, M., Carninci, P., Nishiyama, Y., Hayashizaki, Y., and Shinozaki, K. (1998). High-efficiency cloning of Arabidopsis full-length cDNA by biotinylated CAP trapper. Plant J. **15,** 707–720.

Seki, M., et al. (2002). Functional annotation of a full-length Arabidopsis cDNA collection. Science **296,** 141–145.

Shimada, T., Fuji, K., Tamura, K., Kondo, M., Nishimura, M., and Hara-Nishimura, I. (2003a). Vacuolar sorting receptor for seed storage proteins in *Arabidopsis thaliana.* Proc. Natl. Acad. Sci. USA **100,** 16095–16100.

Shimada, T., Koumoto, Y., Li, L., Yamazaki, M., Kondo, M., Nishimura, M., and Hara-Nishimura, I. (2006). AtVPS29, a putative component of a retromer complex, is required for the efficient sorting of seed storage proteins. Plant Cell Physiol. **47,** 1187–1194.

Shimada, T., Kuroyanagi, M., Nishimura, M., and Hara-Nishimura, I. (1997). A pumpkin 72-kDa membrane protein of precursor-accumulating vesicles has characteristics of a vacuolar sorting receptor. Plant Cell Physiol. **38,** 1414–1420.

Shimada, T., Watanabe, E., Tamura, K., Hayashi, Y., Nishimura, M., and Hara-Nishimura, I. (2002). A vacuolar sorting receptor PV72 on the membrane of vesicles that accumulate precursors of seed storage proteins (PAC vesicles). Plant Cell Physiol. **43,** 1086–1095.

Shimada, T., et al. (2003b). Vacuolar processing enzymes are essential for proper processing of seed storage proteins in *Arabidopsis thaliana.* J. Biol. Chem. **278,** 32292–32299.

Sweet, D.J., and Pelham, H.R. (1992). The *Saccharomyces cerevisiae* SEC20 gene encodes a membrane glycoprotein which is sorted by the HDEL retrieval system. EMBO J. **11,** 423–432.

Sweet, D.J., and Pelham, H.R. (1993). The TIP1 gene of *Saccharomyces cerevisiae* encodes an 80 kDa cytoplasmic protein that interacts with the cytoplasmic domain of Sec20p. EMBO J. **12,** 2831–2840.

Takahashi, H., Saito, Y., Kitagawa, T., Morita, S., Masumura, T., and Tanaka, K. (2005). A novel vesicle derived directly from endoplasmic reticulum is involved in the transport of vacuolar storage proteins in rice endosperm. Plant Cell Physiol. **46,** 245–249.

Takemoto, Y., Coughlan, S.J., Okita, T.W., Satoh, H., Ogawa, M., and Kumamaru, T. (2002). The rice mutant *esp2* greatly accumulates the glutelin precursor and deletes the protein disulfide isomerase. Plant Physiol. **128,** 1212–1222.

Tamura, K., Shimada, T., Kondo, M., Nishimura, M., and Hara-Nishimura, I. (2005). KATAMARI1/MURUS3 is a novel Golgi membrane protein that is required for endomembrane organization in Arabidopsis. Plant Cell **17,** 1764–1776.

Tamura, K., Yamada, K., Shimada, T., and Hara-Nishimura, I. (2004). Endoplasmic reticulum-resident proteins are constitutively transported to vacuoles for degradation. Plant J. **39,** 393–402.

Uemura, T., Ueda, T., Ohniwa, R.L., Nakano, A., Takeyasu, K., and Sato, M.H. (2004). Systematic analysis of SNARE molecules in *Arabidopsis*: Dissection of the post-Golgi network in plant cells. Cell Struct. Funct. **29,** 49–65.

Vitale, A., and Hinz, G. (2005). Sorting of proteins to storage vacuoles: How many mechanisms? Trends Plant Sci. **10,** 316–323.

Watanabe, E., Shimada, T., Kuroyanagi, M., Nishimura, M., and Hara-Nishimura, I. (2002). Calcium-mediated association of a putative vacuolar sorting receptor PV72 with a propeptide of 2S albumin. J. Biol. Chem. **277,** 8708–8715.

Watanabe, E., Shimada, T., Tamura, K., Matsushima, R., Koumoto, Y., Nishimura, M., and Hara-Nishimura, I. (2004). An ER-localized form of PV72, a seed-specific vacuolar sorting receptor, interferes the transport of an NPIR-containing proteinase in Arabidopsis leaves. Plant Cell Physiol. **45,** 9–17.

Xiao, J., Liu, C.C., Chen, P.L., and Lee, W.H. (2001). RINT-1, a novel Rad50-interacting protein, participates in radiation-induced G(2)/M checkpoint control. J. Biol. Chem. **276,** 6105–6111.